Ratcheting of 316L stainless steel thin wire under tension-torsion loading

Sichao Fu, Dunji Yu, Gang Chen, Xu Chen
School of Chemical Engineering and Technology, Tianjin University
fu_sc126@126.com, djyu@tju.edu.cn, agang@tju.edu.cn, xchen@tju.edu.cn

ABSTRACT. A series of cyclic tension-torsion tests under symmetric shear strain and asymmetric axial stress control in various loading paths are conducted on 100 μm-diameter 316L steel wires applying a micro tension-torsion fatigue testing apparatus. The ratcheting strain of the thin wire increases with increasing axial mean stress and decreases in a sequence of linear, rhombic and circular paths. The macro-scale based cyclic plastic constitutive models with kinematic hardening rules of the Ohno-Wang (O-W) and the Chen-Jiao-Kim (C-J-K) are evaluated for the thin wire. Comparing with the O-W, the C-J-K predicts more accurately under high axial stress. While the loading path effects on ratcheting for wire specimens are basically simulated, the macro-based models tend to under-estimate the effect of phase difference between axial and torsional loadings and the ratcheting evolution in the initial 50 cycles.

KEYWORDS. Thin wire; Tension-torsion; Ratcheting; 316L stainless steel.

Citation: Fu, S., Yu, D., Chen, G., Chen, X., Ratcheting of 316L stainless steel thin wire under tension-torsion loading, Frattura ed Integrità Strutturale, 38 (2016) 141-147.

Received: 30.05.2016
Accepted: 25.06.2016
Published: 01.10.2016

INTRODUCTION

Cyclic mechanical behaviors under multiaxial loading conditions at small-scale are key issues in the design of durable micro-devices as well as crucial aspects in characterizing mechanical properties of materials. While the issues at macro-scale have been widely studied for decades, research on multiaxial mechanical properties at micro-scale is quite limited. Most researches on this issue have focused on the biaxial cyclic tensile behaviors of thin films on substrates [1, 2]. Another fundamental multiaxial property, the tension-torsional cyclic behavior, is barely studied experimentally at micro-scale because of the technological problems of precise loading control and measurements. Recently, a novel tension-torsional fatigue apparatus for micro-scale components has been developed [3] and enables the biaxial cyclic tests on thin wires.

In this study, a series of cyclic tension-torsion tests under various loading paths are conducted on 100 μm-diameter 316L stainless steel wires. The material is widely used in micro-devices such as cardiovascular stents. In service, small-scale components may undergo multiaxial loading with tensile stress due to low structural stiffness, leaving multiaxial ratcheting

one concern in the design of stents. The low level ratcheting under biaxial loading is observed and simulated by means of macro-scale based kinematic hardening rules of the Ohno-Wang (O-W) and Chen-Jiao-Kim (C-J-K).

EXPERIMENTAL PROCEDURE

A micro tension-torsional fatigue apparatus for thin wires, as shown in Fig. 1, is applied in this study. The coupled tensile and torsional loading at the scale of 10^0 N-10^2 μNm is achieved by a tensile and a torsional load frame that actuated and measured independently without interfering with each other. A wire specimen is clamped between the frames that have been aligned by an x-y translation stage. A linear motor connected with a load cell is applied in the tensile frame, which allows for the precise control of axial force and the free axial movement of specimen. The micro-torque of the specimen in test is loaded by a DC micro motor and measured by a high precision torque transducer through the transference of a thrust air bearing. The axial deformation of the wire specimen in tension-torsion tests is measured by a grating sensor built in the linear motor and corrected based on data acquired by a non-contact displacement detection system (NDDS) in uniaxial tension tests. More details about this apparatus can be found elsewhere [3].

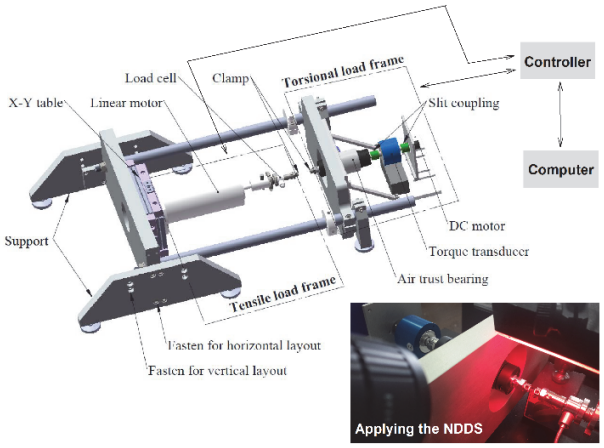

Figure 1: Schematic illustration of the tension-torsional fatigue apparatus for micro-scale components.

The material used in this study is 316L stainless steel soft tempered wire, in nominal diameter of 100 μm, annealed with pure hydrogen. The chemical composition of the material is (wt%): C 0.03%, Cr 16.93%, Ni 12%, Mn 0.95%, P 0.63%, S 0.21%, Mo 2.39%, Si 1%. The actual diameters of specimens were measured before testing by using a scanning electron microscope (SEM). The gauge lengths of the specimens were denoted as the distance between the edges of clamps, which was set to be around 6 mm for all tests. Uniaxial tension tests and torsion tests were conducted to derive the basic mechanical properties.

The cyclic tension-torsion tests were conducted at room temperature under load control for axial loading and angle control for torsional loading. The loading paths in the axial stress-shear strain plane (σ-γ plane) are illustrated in Fig. 2, and test conditions are given in Tab. 1. In all cases the shear strain amplitude is 0.55%. As the strains in this study are small and consist of low level of plasticity, the shear stress is derived with the hypothesis of linear distribution in the cross section. The shear strain and stress are calculated as follows:

$$\gamma = \frac{\theta D}{l} \tag{1}$$

$$\tau = \frac{16T}{\pi D^3} \tag{2}$$

where γ is the shear strain, τ is the shear stress, θ is the twisting angle, T is the corrected torque, and D and l are the diameter and gauge length of wire specimen, respectively. In addition, a completely reserved torsional test with shear strain amplitude of 2% was performed to characterize the isotropic softening behavior of the material. A minimum axial stress of

26 MPa was persisted during the test in order to avoid buckling of the wire specimen. All tests were conducted at a shear strain rate of 0.002/s.

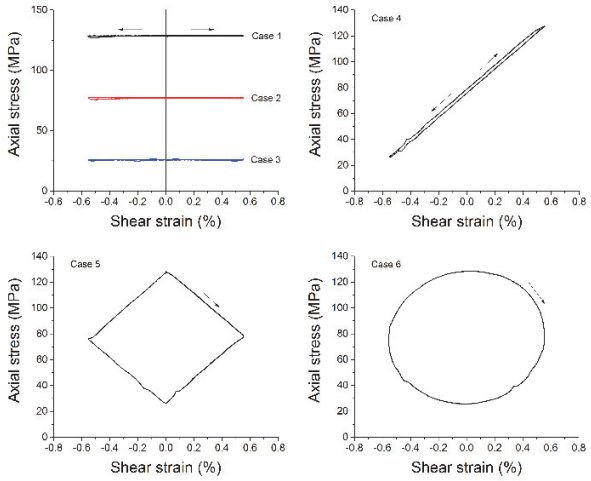

Figure 2: Loading paths in cyclic tension-torsion tests.

Path	$\Delta\gamma / 2$ (%)	γ_{mean} (%)	$\Delta\sigma / 2$ (MPa)	σ_{mean} (MPa)
Case 1	0.55	0	0	128
Case 2	0.55	0	0	77
Case 3	0.55	0	0	26
Case 4	0.55	0	51	77
Case 5	0.55	0	51	77
Case 6	0.55	0	51	77

Table 1: Multiaxial ratcheting testing of 316L wire under various loading paths

EXPERIMENTAL RESULTS

Fig. 3 shows the experimental results of Case 4 under linear path. The shear hysteresis loop exists as shown in Fig. 3(a). The accompanied tensile stress, reversed between 26 and 128 MPa and far below the 0.2% yield strength, contributes to an asymmetric stress state (Fig. 3(d)) that leads to ratcheting in the axial direction. The remarkable axial strain accumulation is demonstrated in the axial stress-strain curve (Fig. 3(b)) as well as the strain path (Fig. 3(c)).
The evolution of ratcheting under various loading paths are displayed in Fig. 4. The ratcheting strain is defined as the maximum strain per cycle. With increasing cycle number, the ratcheting strain sharply rises in the beginning and then is slowly suppressed until a stable rate of increment is reached. Case 1 with constant axial stress of 128 MPa displays the highest level of ratcheting. As reducing the axial mean stress, the ratcheting strain decreases and the rate of stable increment after 100 cycles slightly changes. The effect of loading path on ratcheting is demonstrated by case 4-6 with the same range of cycling axial stress. The linear path in case 4 leads to larger ratcheting than the rhombic path in case 5 and the circular path in case 6. The ratcheting behaviors of the rhombic and the circular paths are similar, with the latter slightly lower in value. The deviation caused by loading path is consistent with the multiaxial ratcheting behavior of steels at macro-scale, which is related with the non-proportionality of certain loading path and the resulted additional hardening [6, 7].

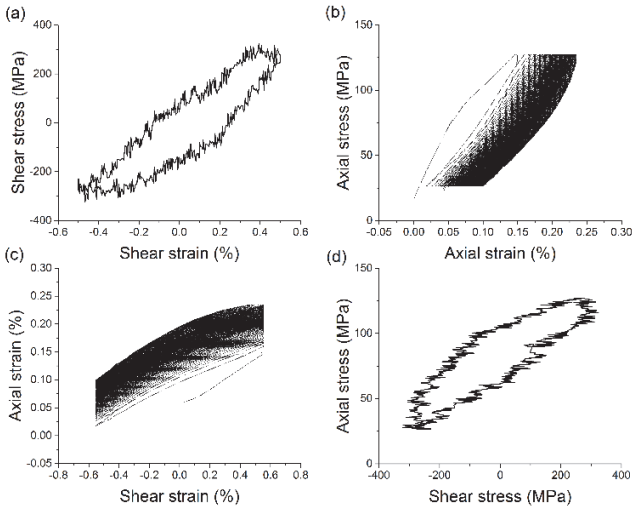

Figure 3: Experimental results of case 4, (a) shear stress-strain curve in cycle 200, (b) axial stress-strain curve, (c) strain path and (d) stress path in cycle 200.

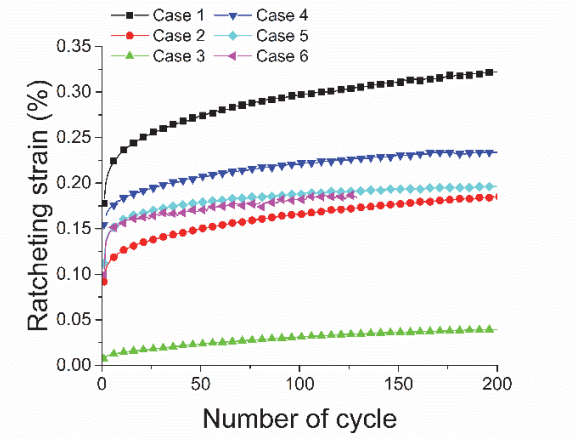

Figure 4: Evolution of ratcheting strain under various loading path

EVALUATION OF MACRO-SCALE BASED CYCLIC PLASTICITY

The macro-scale based cyclic plasticity with the assumption of rate-independent material's behavior is phenomenologically described by three parts: yield criterion, plastic flow rule and the kinematic hardening rule. The kinematic hardening rule is the central part of the constitutive modelling of cyclic plasticity. It defines the translation of yield surface in stress space during plastic deformation, which is the most important feature for the multiaxial ratcheting simulation. Two of the most successful kinematic hardening rules are evaluated for the ratcheting simulation of 316L thin wires: the nonlinear Ohno and Wang (O-W) [8] and the Chen-Jiao-Kim (C-J-K) [6] rules.

$$\text{O-W:}\quad a=\sum_1^M a_i,\quad da_i=\gamma_i\left[\frac{2}{3}r_i d\varepsilon_p-\left(\frac{\overline{a_i}}{r_i}\right)^{m_i}\left\langle d\varepsilon_p\cdot\frac{\underline{\underline{a_i}}}{a_i}\right\rangle a_i\right] \tag{3}$$

$$\text{C-J-K:}\quad da_i=\gamma_i\left[\frac{2}{3}r_i d\varepsilon_p-\left\langle n\cdot\frac{\underline{\underline{a_i}}}{a_i}\right\rangle^{\chi_i}\left(\frac{\overline{a_i}}{r_i}\right)^{m_i}\left\langle d\varepsilon_p\cdot\frac{\underline{\underline{a_i}}}{a_i}\right\rangle a_i\right] \tag{4}$$

where a_i is the ith component of back stress a, $\overline{a_i}$ is the magnitude of a_i, ε_p is the plastic strain tensor, γ_i, r_i and m_i are material constants (i = 1, 2, … M), n is the direction of plastic strain rate or the normal vector of yield surface, χ_i is a multiaxial parameter. $\langle\ \rangle$ is the Macauley bracket: $\langle A\rangle = A$ if $A > 0$, $\langle A\rangle = 0$ otherwise.

The total back stress in this study is decomposed into 8 components for the O-W and C-J-K rules. All the γ_i and r_i components in the O-W are determined from a torsion test by the scheme discussed by Bari and Hassan [9]. m_i is determined from a tension-torsion test which is low in stress ratio $\sigma_{\max} / \tau_{\max}$. The χ_i introduced in the C-J-K is selected by calibrating with a tension-torsion test with low axial stress. The values of the parameters are: $\sigma_0 = 200$ MPa; $\gamma_{1\sim8} = 5000$, 1000, 311.7, 161.6, 51.3, 15.2, 5.2, 3.2; $r_{1\sim8} = 180$, 90, 140, 18, 7.6, 48.7, 200, 132 MPa; $m_i (i = 1 \sim 8) = 10$; $\chi_i (i = 1 \sim 8) = 3$;. The predicted cyclic stress-strain response of case 4 in linear path by the C-J-K is illustrated in Fig. 5. The O-W and the C-J-K rule predict similar response of shear stress and axial strain in this case. Obvious shear hysteresis loop and axial ratcheting behavior is appropriately simulated.

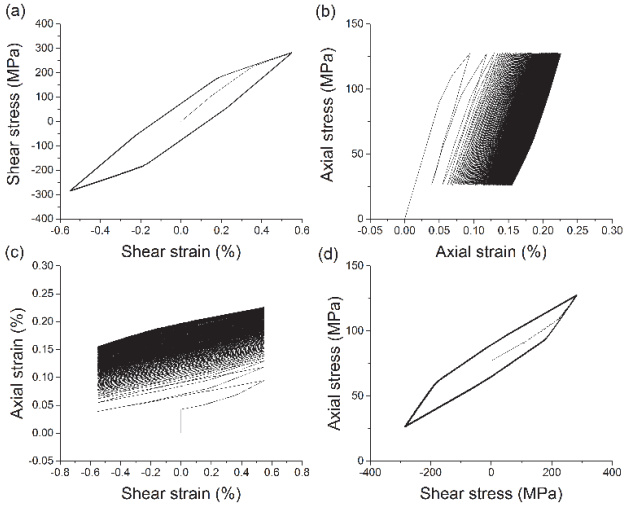

Figure 5: Predicted results of case 4 under linear path by the C-J-K, (a) shear stress-strain curve, (b) axial stress-strain curve, (c) strain path and (d) stress path.

The ratcheting responses obtained by the O-W and the C-J-K models as well as experimental data are presented in Fig. 6. The O-W and the C-J-K predicted similar ratcheting evolutions with small errors for cases 2-6. In terms of case 1 with relatively high axial mean stress, the O-W obviously over-predicts as the non-proportionality of loading increases. By taking into account the non-coaxiality of plastic strain rate for reducing dynamic recovery, the C-J-K successfully suppresses the ratcheting under relatively high non-proportional hardening in case 1.

Comparing with simulations for cases 1-3 with constant axial stresses, the C-J-K or the O-W model predicted with more errors for cases 4-6 with loading-unloading axial stress, especially for cases 5, 6 with phase differences of tensile and torsional loading. While the models under-estimate the ratcheting evolution under linear path in case 4, they over-predict ratcheting under rhombic path in case 5 and circular path in case 6. Thus it is suggested that the phase difference of loading in two directions has more influence on ratcheting than that predicted by the models.

Deficiency of simulation also exists in the initial ratcheting stage with high but sharply decreased strain rate. The experimental ratcheting evolves more dramatically with larger decreasing rate in this stage than simulation, which results in the under-predictions within about 50 cycles in most cases. The quickly retarded ratcheting may implies some additional hardening related with plastic strain gradients that prominent in small-scale components undergoing inhomogeneous deformation such as torsion or bending. Under an applied torque, while one dislocation of a dipole moves outward and escape or annihilated, another dislocation moves inward under stress gradients and piles up around the wire center, which results in polarized dislocations (or GNDs) with non-uniform density [10]. The inhomogeneous spatial distribution of GNDs, or the resulted plastic strain gradients, can lead to a strong back stress [5] and may suppress the multiaxial ratcheting of thin wire. Further work on the microstructure observation is needed to clearly explain the multiaxial ratcheting behavior

at small-scale. And the models may be modified to give phenomenological predictions for ratcheting in engineering applications.

Though certain difference exists between simulation and experimental data, the effects of loading paths on ratcheting is basically described by both models, that is, the ratcheting strain increases with increasing mean stress and reduces with non-proportionality in a sequence of linear>rhombic>circular paths.

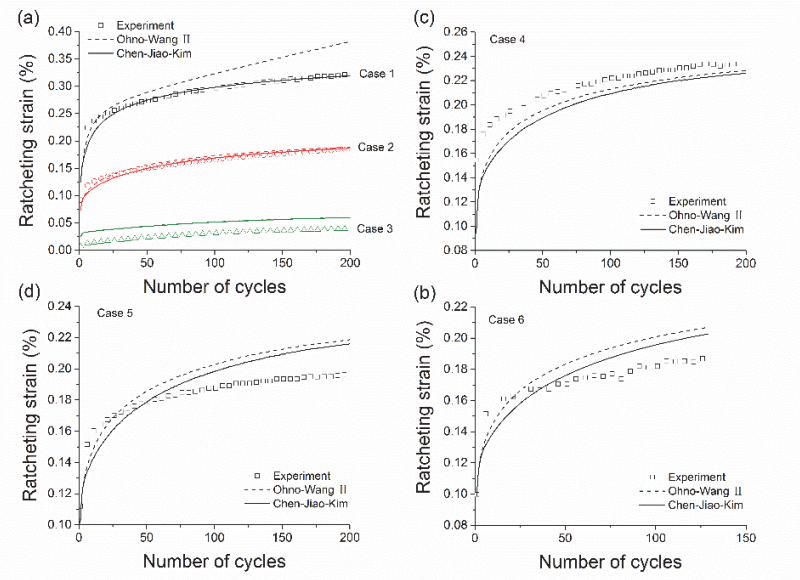

Figure 6: Ratcheting strain predicted by the O-W and the C-J-K models, (a) cases 1-3 under constant axial stress, (b) case 4 under linear path, (c) case 5 under rhombic path, (d) case 6 under circular path.

Conclusion

The ratcheting strain of 100 μm-diameter 316L wire increases with increasing axial mean stress and decreases in a sequence of linear, rhombic and circular paths, which suggests similar effect of loading paths on ratcheting of the micro-scale components with that of bulk material. The C-J-K predicts more accurately than the O-W under relatively high axial stress. Both models basically simulate the loading path effect on ratcheting for wire specimens. However, the models tend to under-estimate the effect of phase difference between axial and torsional loadings. And the experimental ratcheting strain evolves more dramatically with larger decreasing rate than prediction in the initial 50 cycles, which may imply some additional hardening related with plastic strain gradients.

Acknowledgments

The authors are grateful for the financial support from the National Natural Science Foundation of China (Nos. 11372215 and 51435012).

References

[1] Alaca, B. E., Selby, J. C., Saif, M. T. A., Sehitoglu, H., Biaxial testing of nanoscale films on compliant substrates: Fatigue and fracture, Rev. Sci. Instrum., 73 (2002) 2963.

[2] Baker, S. P., Keller-Flaig, R. M., Shu, J. B., Bauschinger effect and anomalous thermomechanical deformation induced by oxygen in passivated thin Cu films on substrates, Acta Mater., 51 (2003) 3019-3036.

[3] Fu, S., Wang, L., Chen, G., Yu, D., Chen, X., A tension-torsional fatigue testing apparatus for micro-scale components, Rev. Sci. Instrum., 87 (2016) 015111.
[4] Yang, X., Gao, Q., He, G., Cai, L., On nonproportional cyclic properties of type 316 stainless steels, Acta Metallurgica Sinica, 32 (1996) 15-22.
[5] Liu, D., He, Y., Shen, L., Lei, J., Guo, S., Peng, K., Accounting for the recoverable plasticity and size effect in the cyclic torsion of thin metallic wires using strain gradient plasticity, Mater. Sci. Eng. A, 647 (2015) 84-90.
[6] Chen, X., Jiao, R., Kim, K.S., On the Ohno-Wang kinematic hardening rules for multiaxial ratcheting modeling of medium carbon steel, Int. J. Plasticity, 21 (2005) 161-184.
[7] Hamidinejad, S.M., Varvani-Farahani, A., Ratcheting of 304 stainless steel under multiaxial step-loading conditions, Int. J. Mech. Sci., 100 (2015) 80-89.
[8] Ohno, N., Wang, J.-D., Kinematic hardening rules with critical state of dynamic recovery, part I: formulation and basic features for ratcheting behavior, Int. J. Plasticity, 9 (1993) 375-390.
[9] Bari, S., Hassan, T., Anatomy of coupled constitutive models for ratcheting simulation, Int. J. Plasticity, 16 (2000) 381-409.
[10] Liu, D., He, Y., Dunstan, D. J., Zhang, B., Gan, Z., Hu, P., Ding, H., Toward a further understanding of size effects in the torsion of thin metal wires: An experimental and theoretical assessment, Int. J. Plasticity, 41 (2013) 30-52.